

# Universality of scaling entropy in charged hadron multiplicity distributions at the LHC

L.S. Moriggi<sup>1\*</sup>

<sup>1</sup> *Universidade Estadual do Centro-Oeste (UNICENTRO), Campus Cedeteg, Guarapuava 85015-430, Brazil*

F. S. Navarra<sup>†</sup>

*Instituto de Física, Universidade de São Paulo, Rua do Matão,  
1371, CEP 05508-090, Cidade Universitária, São Paulo, SP, Brazil.*

M.V.T. Machado<sup>2‡</sup>

<sup>2</sup> *High Energy Physics Phenomenology Group, GFPAE. Institute of Physics,  
Federal University of Rio Grande do Sul (UFRGS)  
Caixa Postal 15051, CEP 91501-970, Porto Alegre, RS, Brazil*

In this work, we investigate the scaling behavior of the entropy associated with the charged hadron multiplicity distribution  $P(N)$  in proton–proton collisions at the LHC. We show that the growth of this entropic indicator as a function of the Bjorken- $x$  variable exhibits a universal behavior, consistent with observations from deep inelastic scattering (DIS). This universality suggests that the entropy scaling is a property of the initial state and reflects the diffusive nature of gluon dynamics at small  $x$ . Furthermore, we demonstrate that high-multiplicity events are not accurately described by traditional KNO scaling and require a more precise description based on a diffusion scaling framework. This new scaling emerges naturally from the universal growth of partonic entropy and offers a deeper insight into the dynamics of particle production in high-energy hadronic collisions.

## I. INTRODUCTION

Understanding the probability distribution  $P(N)$  for producing  $N$  charged hadrons in high-energy collisions is fundamental to unraveling the dynamics of quarks and gluons during the initial and final stages of the collision process. Although  $P(N)$  is one of the most extensively studied observables in high-energy physics, recent LHC data have pushed the limits of our theoretical understanding. In particular, *high-multiplicity events* — in which the number of produced particles greatly exceeds the mean — reveal significant discrepancies between theoretical predictions and experimental observations. These large fluctuations challenge conventional QCD expectations and expose tensions between standard event generators and data, not only in proton-proton ( $pp$ ) but also in heavy-ion ( $AA$ ) collisions.

The spectral shape of charged hadrons exhibits a strong dependence on event multiplicity, in a manner incompatible with existing QCD-inspired models and event generators [1]. Specifically, the variation of transverse momentum ( $p_T$ ) spectra across multiplicity classes leads to behaviors that are difficult to reconcile with current theoretical frameworks.

Without a proper theoretical control of multiplicities in  $pp$  collisions, it becomes increasingly unrealistic to interpret final-state observables in heavy-ion collisions with confidence. In fact, phenomena traditionally attributed

to quark-gluon plasma (QGP) formation may originate from a lack of understanding of the underlying gluon dynamics in the initial state. A recent ALICE study on multiplicities in  $p$ -Pb collisions [2] reveals large discrepancies between data and predictions from widely used Monte Carlo event generators. It also shows incompatibility with the GLASMA model [3], highlighting serious limitations in current theoretical approaches. Moreover, several QGP-like signals observed in  $AA$  collisions are now being detected in small systems like  $pp$  and  $p$ -Pb collisions [2], raising fundamental questions about their true origin. This convergence of phenomena across system sizes constitutes one of the most urgent open problems in high-energy hadron physics.

The multiplicity distributions measured by ALICE at different center-of-mass energies exhibit significant deviations from the *Koba-Nielsen-Olesen (KNO) scaling* [4], particularly in the tails of the distribution where  $N/\langle N \rangle > 4$  [5]. These deviations grow with increasing collision energy and are most pronounced in the high-multiplicity regime, where rare events dominate. The violation of KNO scaling reflects a breakdown of self-similarity and suggests the emergence of new dynamical scales not accounted for in early scaling hypotheses.

Various theoretical frameworks have been proposed to describe these deviations, including negative binomial distributions (NBDs) with soft and semi-hard components [6] and multi-component models [7]. While these approaches offer reasonable phenomenological fits, they typically involve a large number of free parameters that lack a clear interpretation in QCD and often exhibit inconsistent behavior when analyzed across different kinematic regimes.

---

\* e-mail: lucasmoriggi@unicentro.br

† e-mail: navarra@if.usp.br

‡ e-mail: magnus@if.ufrgs.br

The CMS Collaboration also investigated KNO scaling at different pseudorapidity windows [8], showing stronger violations in broader rapidity intervals and at higher multiplicities. A comprehensive ATLAS study over a wide energy range ( $\sqrt{s} = 0.9$  to 13 TeV) [9] confirmed that KNO violations become increasingly significant at lower energies and large multiplicities.

These findings raise several open questions:

- Are the apparent collective effects in small systems the result of final-state interactions or do they reflect intrinsic initial-state dynamics, such as gluon saturation?
- Can a universal scaling behavior be established across different collision systems, such as  $ep$ ,  $pp$ , and  $AA$ ?
- What mechanisms govern the rare, large-multiplicity events found in the tails of  $P(N)$ ?
- Is KNO scaling a fundamental feature, or should it be replaced by a more general scaling law?

While a fully robust theoretical framework is still lacking, the idea of *scaling laws* provides a promising bridge between empirical regularities in the data and theoretical models rooted in partonic dynamics. One such approach is based on *small- $x$  scaling*, motivated by gluon saturation models. In this picture, the gluon distribution reaches a saturation scale  $Q_s$ , which governs the typical transverse momentum and particle multiplicity. Evidence of such scaling behavior has been observed in inclusive particle production at both HERA [10–14] and the LHC [14–19].

In [15, 20], a new observable called *scaling entropy* was introduced, proposed as a consequence of the universal growth of gluon distributions at small Bjorken- $x$ , resulting in the functional form:

$$S(x) = \lambda \log(1/x) + \text{const.}$$

Remarkably, the entropy extracted from the charged hadron multiplicity distribution in deep inelastic scattering (DIS) agrees with this prediction, and the growth exponent  $\lambda$  has been measured directly from data.

In this study, we investigate the implications of *scaling entropy* in the context of multiplicity distributions at the LHC. We perform a phenomenological analysis of probability distribution  $P(N)$  from ALICE, CMS, and ATLAS data. We demonstrate that, after subtracting the soft component of the spectrum, the entropy of hadron production in  $pp$  collisions exhibits scaling behavior consistent with that found in HERA  $ep$  data. This suggests the presence of universal initial-state dynamics governing particle production.

As a consequence of this behavior, we argue that *KNO scaling* must be replaced with a more accurate *diffusion scaling*, which naturally emerges from the universal growth of parton distributions and entropy in the initial

state. This new perspective offers a path toward a deeper understanding of high-multiplicity events and their connection to fundamental QCD dynamics.

## II. THEORETICAL FRAMEWORK AND MAIN PREDICTIONS

In the dipole picture of deep inelastic scattering (DIS) [21], the internal structure of the proton is probed via the scattering of a virtual photon. This process can be factorized into the convolution of the photon wave function and a dipole-target scattering amplitude  $\mathcal{N}(x, r)$ , resulting in the total cross section:

$$\sigma_{\gamma^*p}(x, Q^2) = \sigma_0 \int d^2\mathbf{r} dz |\psi_\gamma(r, z)|^2 \mathcal{N}(x, r), \quad (1)$$

where  $\mathbf{r}$  is the transverse size of the dipole,  $z$  is the longitudinal momentum fraction carried by the quark, and  $\psi_\gamma(r, z)$  is the photon light-cone wave function.

The scattering amplitude  $\mathcal{N}(x, r)$  must respect unitarity in position space, i.e.,  $\mathcal{N}(x, r) \leq 1$ , which ensures the saturation of interaction probability at large  $r$ . This leads to the emergence of a dynamical scale known as the *saturation scale*,  $Q_s(x)$ , which marks the transition between dilute and dense partonic systems and is a decreasing function of Bjorken- $x$ .

In momentum space  $k_T$ , the unitarity constraint manifests as the growth of the variance of the transverse momentum distribution with decreasing  $x$ . In a parton cascade picture, emissions follow an evolution where the characteristic time scale is governed by the uncertainty principle,  $t \sim 1/x$ , leading to anomalous diffusion in transverse momentum space:

$$\langle k_T^2(x) \rangle \sim \left( \frac{1}{x} \right)^\lambda, \quad (2)$$

where  $\lambda$  is related to the *hard Pomeron intercept*, characterizing the rate of growth of partonic activity and gluon density at small  $x$ .

Even without detailed knowledge of the exact form of the probability distribution  $\mathcal{P}(x, k_T^2)$ , the evolution of the diffusion front satisfies the following scaling form:

$$\mathcal{P}(x, k_T^2) \sim \frac{1}{x^{-\lambda}} f\left(\frac{k_T^2}{x^{-\lambda}}\right). \quad (3)$$

The entropy associated with the initial-state partonic distribution is defined by:

$$S^{\text{parton}}(x) = - \int \mathcal{P}(x, k_T) \log[\mathcal{P}(x, k_T)] d^2k_T. \quad (4)$$

Under the scaling form (3), the entropy takes on a universal logarithmic behavior:

$$S^{\text{parton}}(x) = C + \lambda \log\left(\frac{1}{x}\right), \quad (5)$$

where the constant  $C$  encodes all the model-dependent details of  $\mathcal{P}$ , and the  $\lambda \log(1/x)$  term reflects a universal scaling behavior associated with the growth of gluon densities.

Experimentally, we can define a related observable from the multiplicity distribution of charged hadrons:

$$S^{\text{mult}} = - \sum_N P(N) \log P(N), \quad (6)$$

where  $P(N)$  is the probability of producing  $N$  charged hadrons in a given event class.

In  $pp$  collisions,  $S^{\text{mult}}$  depends on the pseudorapidity interval  $\eta$  in which the measurement is performed and on the center-of-mass energy  $\sqrt{s}$  of the collision. The relevant Bjorken- $x$  value for the partonic subprocess can be estimated from the minimal transverse momentum  $p_T$  and the pseudorapidity of the produced particles:

$$x_{a,b} = \frac{p_T}{\sqrt{s}} e^{\pm\eta}. \quad (7)$$

Since most partonic interactions occur at low  $x$ , the effective value of  $x$  for the subprocess is approximately:

$$x \approx \frac{e^{-\eta}}{\sqrt{s}}, \quad (8)$$

assuming  $p_T \sim 1$  GeV for soft-scale interactions.

Substituting this into Eq. (5), we can write a phenomenological scaling form for the experimentally measured entropy:

$$S^{\text{mult}}(\sqrt{s}, \eta) = \lambda \log\left(\frac{1}{x}\right) + f(\eta), \quad (9)$$

where the first term depends only on the initial-state gluon dynamics through  $x$ , and the second term  $f(\eta)$  may include contributions from hadronization and final-state effects independent of  $\sqrt{s}$ . This scaling hypothesis provides a quantitative approach to test the principle of *local parton-hadron duality* [22], which posits that final-state hadron distributions closely reflect initial partonic configurations.

In DIS, Eq. (5) can be directly tested thanks to the hard scale  $Q^2$ . In contrast, LHC data are often collected with low  $p_T$  cuts, where soft physics contributions may obscure the scaling behavior. To mitigate this, we divide particle production into two components: a soft component dominant at low multiplicities ( $N < N_{\min}$ ) and a semi-hard component dominant at high multiplicities ( $N > N_{\min}$ ). Scaling behavior is expected only in the latter.

While there is no universal definition for  $N_{\min}$ , our analysis (to be shown in the next section) reveals that for  $N_{\min} \sim 10$ , the extracted growth rate  $\lambda$  stabilizes and becomes consistent with that observed in HERA DIS data, i.e.,  $\lambda_{\text{LHC}} = \lambda_{\text{H1}}$ . This observation supports the universality of the entropy growth law across different collision systems.

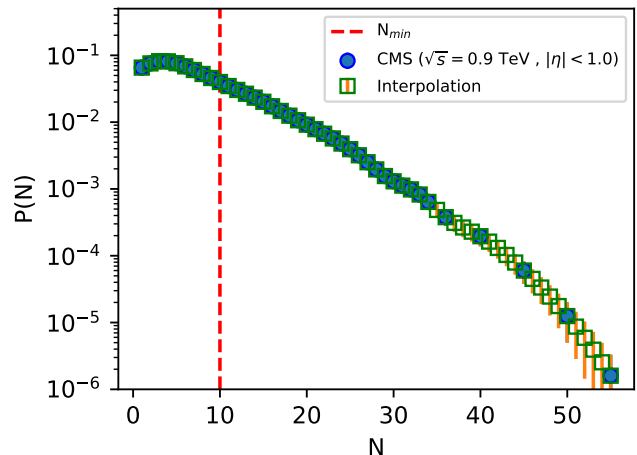


FIG. 1: Multiplicity data (full box) and interpolated values (unfill) at some  $N$  bins. The vertical line shows the cut imposed of  $N_{\min} = 10$ .

To quantify fluctuations, we also consider the variance of the multiplicity distribution:

$$\text{Var}(N) = \sum (N - \langle N \rangle)^2 P(N). \quad (10)$$

The central goal of this work is to confront the theoretical prediction of parton scaling entropy in Eq. (5) with the experimentally measured multiplicity entropy in Eq. (6), and to investigate whether a universal scaling behavior underlies particle production in high-energy hadron collisions.

### III. RESULTS AND DISCUSSIONS

#### IV. RESULTS

Different LHC collaborations adopt distinct methodologies for extracting the charged hadron multiplicity distribution  $P(N)$ , often applying different kinematic cuts, pseudorapidity windows, and transverse momentum thresholds. For this analysis, we compiled data from CMS, ALICE, and ATLAS across several center-of-mass energies  $\sqrt{s}$  and pseudorapidity intervals  $\eta$ , when available. We define four data sets for comparison:

- **Set 1:** CMS data [8] with a large rapidity window, divided in five intervals from  $\eta_{\max} = 0.5$  to  $\eta_{\max} = 2.5$ . Non-single-diffractive (NSD) events were selected using a minimum-bias trigger and a lower  $p_T$  threshold of 0.1 GeV. Each rapidity window is given for different values of  $\sqrt{s}$ .
- **Set 2:** ATLAS data [9, 23, 24] with a large rapidity window of  $\eta_{\max} = 2.5$ . Events were collected using a single-arm minimum-bias trigger, with selections to reduce diffractive contributions. Only charged

TABLE I: Extracted  $\lambda$  values from different LHC data sets at various pseudorapidity windows and center-of-mass energies.

Data Set	$p_T$ threshold (GeV)	$\eta_{\max}$	$\sqrt{s}$ (GeV)	$\lambda \pm \Delta\lambda$	$\chi^2/\text{dof}$
1 - CMS	0.1	0.5	900, 2360, 7000	$0.32 \pm 0.02$	0.0003
1 - CMS	0.1	1.0	900, 2360, 7000	$0.34 \pm 0.02$	0.0098
1 - CMS	0.1	1.5	900, 2360, 7000	$0.33 \pm 0.02$	0.0179
1 - CMS	0.1	2.0	900, 2360, 7000	$0.32 \pm 0.02$	0.0058
1 - CMS	0.1	2.5	900, 2360, 7000	$0.32 \pm 0.02$	0.0003
2 - ATLAS	0.1	2.5	2760, 900, 7000, 8000, 13000	$0.32 \pm 0.01$	1.1045
3 - ALICE	0.15	0.8	2760, 5020, 7000, 8000, 13000	$0.32 \pm 0.01$	0.9907
4 - ALICE	0.05	0.5	900, 2760, 7000, 8000	$0.29 \pm 0.03$	0.4514
4 - ALICE	0.05	1.0	900, 2760, 7000, 8000	$0.30 \pm 0.02$	0.4980
4 - ALICE	0.05	1.5	900, 2760, 7000, 8000	$0.29 \pm 0.01$	0.5657

particles with transverse momentum  $p_T > 0.1$  GeV were included. [20]:

$$\lambda_{\text{DIS}} = 0.322 \pm 0.007. \quad (11)$$

- **Set 3:** ALICE data [25], Inclusive primary charged particles with  $0.15 \text{ GeV} < p_T < 10 \text{ GeV}$  were measured in a narrow pseudorapidity range of  $\eta_{\max} = 0.8$ .
- **Set 4:** ALICE data [5] at extended rapidity coverage at different values of pseudorapidity from 0.5 to 1.5. Non single diffractive events with lower  $p_T$  threshold of approximated 0.05 GeV.

Due to differences in analysis techniques and  $p_T$  thresholds, the multiplicity distributions in these sets are not directly comparable. A summary of the experimental characteristics and cuts applied is presented in Table I.

In some cases (notably CMS), the  $P(N)$  values are not reported for all consecutive values of  $N$ , which prevents direct computation of the entropy via Eq. (6). To address this, we perform a smooth interpolation using exponential cubic splines to estimate missing points and associated uncertainties. The procedure is illustrated in Fig. 1, where the interpolated bins are shown unfilled and a vertical dashed line indicates the cutoff value  $N_{\min}$  applied to exclude soft contributions.

In ALICE Set 3 data, the available  $N$  range is limited. To ensure convergence in entropy calculations, we extrapolate the high- $N$  tail of the distribution, which typically contributes about 5% to the total entropy at  $\sqrt{s} = 0.9$  TeV but significantly impacts the extracted value of  $\lambda$ . These preprocessing steps standardize the data sets for meaningful comparison.

We then fit the experimental entropy  $S^{\text{mult}}$  to the scaling form in Eq. (9), assuming a logarithmic dependence on  $x$  for fixed  $\eta$ . The fit extracts the entropy growth rate  $\lambda$  for each pseudorapidity interval. Results for Sets 1 and 2 are shown in Fig. 2, where they are compared with the entropy extracted from deep inelastic scattering data [20].

We observe that the extracted values of  $\lambda$  across different LHC datasets and pseudorapidity windows are consistent, within uncertainties, with the DIS reference value

In particular, the CMS data at  $\sqrt{s} = 0.9$  TeV for the most central pseudorapidity range yields entropy values nearly identical to those in DIS. At larger rapidity windows, entropy increases with  $\sqrt{s}$ , but the rate  $\partial S / \partial \log(1/x)$  remains consistent with the universal value  $\lambda$ . This suggests that, despite experimental differences in  $P(N)$  extraction, the underlying entropy growth rate is a robust feature of QCD dynamics:

$$\frac{\partial S}{\partial \log(1/x)} = \lambda. \quad (12)$$

Next, we analyze ALICE Sets 3 and 4 separately as presented in Fig. 3. Set 3 (central rapidity) shows good agreement with  $\lambda_{\text{DIS}}$ , while Set 4 (extended rapidity) exhibits slightly smaller entropy growth rates, around 7% lower than the other data sets. We believe that the difference is due to lower  $p_T$  thresholds in Set 4, which allows for more soft events. Nevertheless, internal consistency is observed within the ALICE measurements at different  $\eta$ .

An important complementary observable is the variance of the multiplicity distribution. For example, in the case of the negative binomial distribution (NBD), the variance is given by:

$$\text{Var}(N) = \langle N \rangle^2 + \frac{\langle N \rangle^2}{k}, \quad (13)$$

where  $k$  is the shape parameter, and both  $\langle N \rangle$  and  $k$  can vary with  $x$ . Thus, NBD-based models imply that both variance and entropy encode information about partonic dynamics.

Figure 4 shows the variation from the mean, quantified by the square root of the variance and entropy. We observe the linear behavior  $S = \log(\sqrt{\text{Var}(N)}) + \text{cte}$ . This indicates that fluctuations are the dominant source of entropy and that the entropy effectively captures the spread of the parton distribution in momentum space.

Under the diffusion scaling hypothesis, the probability distribution for gluon  $k_T$  diffusion suggests a connection

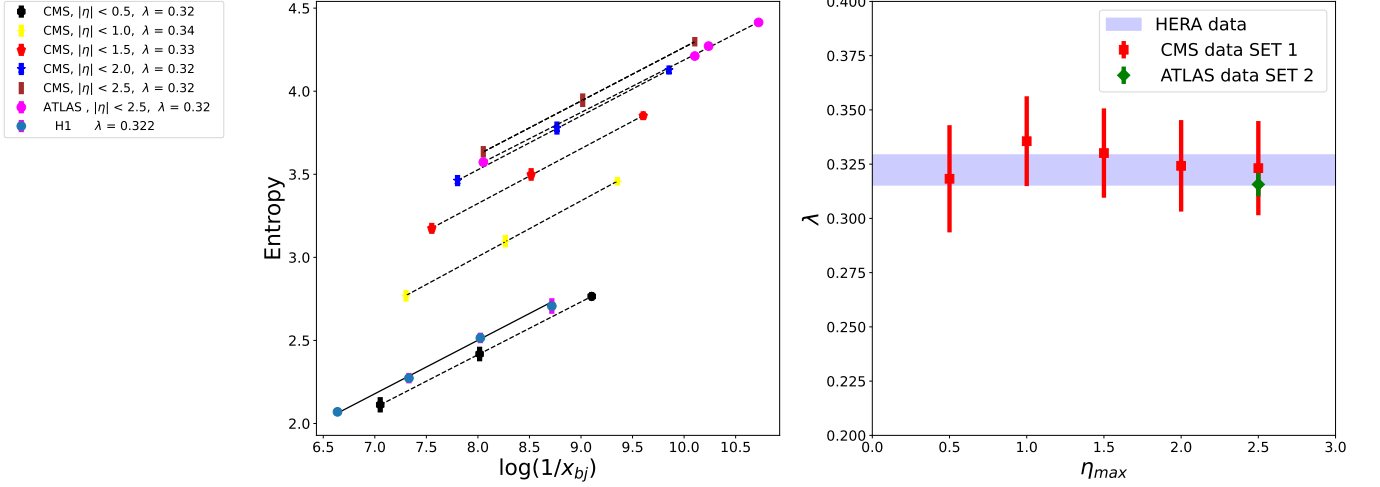


FIG. 2: Left side: Experimental entropy (color bars) compared with scaling entropy line as a function of  $\log(1/x)$  in each rapidity bin when available. The full lines correspond to DIS entropy determined from H1 data. Right: resulting  $\lambda$  compared with blue interval corresponding from H1 fit uncertainty.

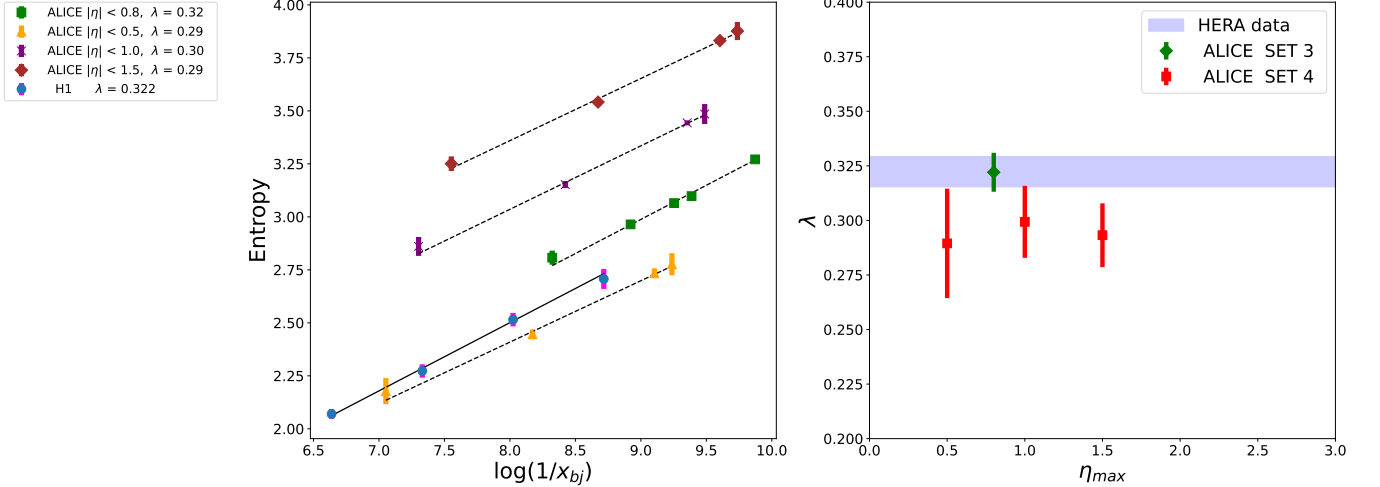


FIG. 3: The same as Fig. 2 for the Sets 3 and 4.

between entropy, variance, and initial-state  $x$  scaling. By analogy, the multiplicity distribution  $P(N)$  is expected to obey:

$$P(N) \sim \frac{1}{x^\lambda} F\left(\frac{(N - \langle N \rangle)}{x^\lambda}\right), \quad (14)$$

where  $F$  is a universal scaling function. Figure 5 shows the diffusion scaling behavior for all data sets analyzed, confirming the remarkable universality of this scaling form across different experiments and kinematic regimes.

Additionally, we compare the traditional KNO scaling with the proposed diffusion scaling using ATLAS data [9, 23, 24]. Figure 6 demonstrates that KNO scaling fails in the high-multiplicity tail ( $N \gg \langle N \rangle$ ), while diffusion scaling remains valid. The comparison is shown for multiple values of  $N_{min}$ , and we find that the diffusive behavior becomes more evident when soft events are

excluded. Notably, KNO scaling appears more reliable at lower multiplicities, suggesting that large fluctuations originate from partonic systems exhibiting diffusion-like behavior rather than self-similar scaling.

The violation of the KNO scaling is interesting. In the context of the Color Glass Condensate, the KNO scaling is related to the multiplicity distributions of soft gluons. It was shown in Ref. [26] that an approximately Gaussian effective theory (with running coupling evolution) describing color charge fluctuations at scales  $\sim Q_s$  is able to reproduce the scaling. In special, the NBD distribution can be derived from this small- $x$  framework [26, 27]. The role played by the selection of the transverse momentum  $p_T$  of produced charged particles within jets has been investigated recently in Ref. [28]. Based on the ATLAS data, it has been shown that the low  $p_T$  region

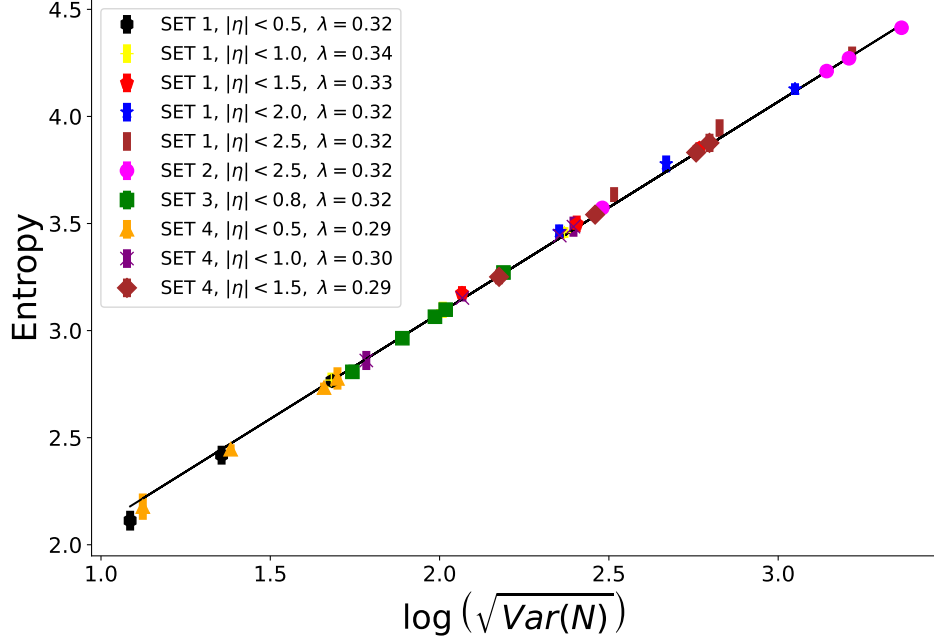


FIG. 4: Entropy as a function of the dispersion to each data set. The full line is a linear global fit.

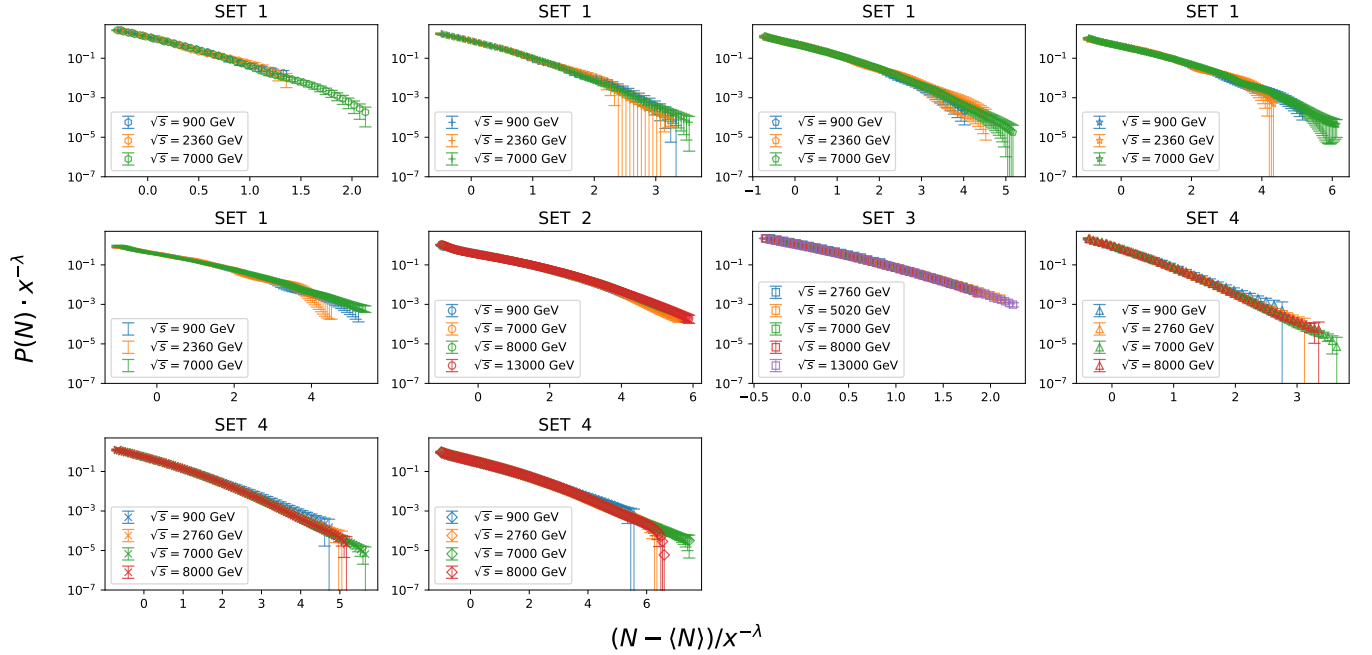


FIG. 5: Each data set scaling line at different rapidities.

does not show KNO scaling, and the higher  $p_T$  range slowly moves toward the scaling. On the other hand, all data can be described by a sub-Poissonian distribution with a distinct  $\delta$  parameter appearing in the birth rate  $\mu_n$  in the cascade equations when the multiplicity is  $n$ ,  $\mu_n = \lambda(n+1)^{-\delta} + \sigma$ . The different  $\delta$  values from the fits suggest that the various transverse momentum ranges are driven by heterogeneous dynamics. Concerning high- $p_T$

jets, there is a general consensus that the double logarithmic approximation (DLA) calculations in pQCD are able to describe the observed KNO scaling [29–31].

In an approach closest to ours, proposed by Levin and collaborators [32–35], the multiplicity distribution is related to the entanglement entropy of gluons in maximally entangled states. In the framework of the parton model, the high energy multiplicity distribution has the follow-

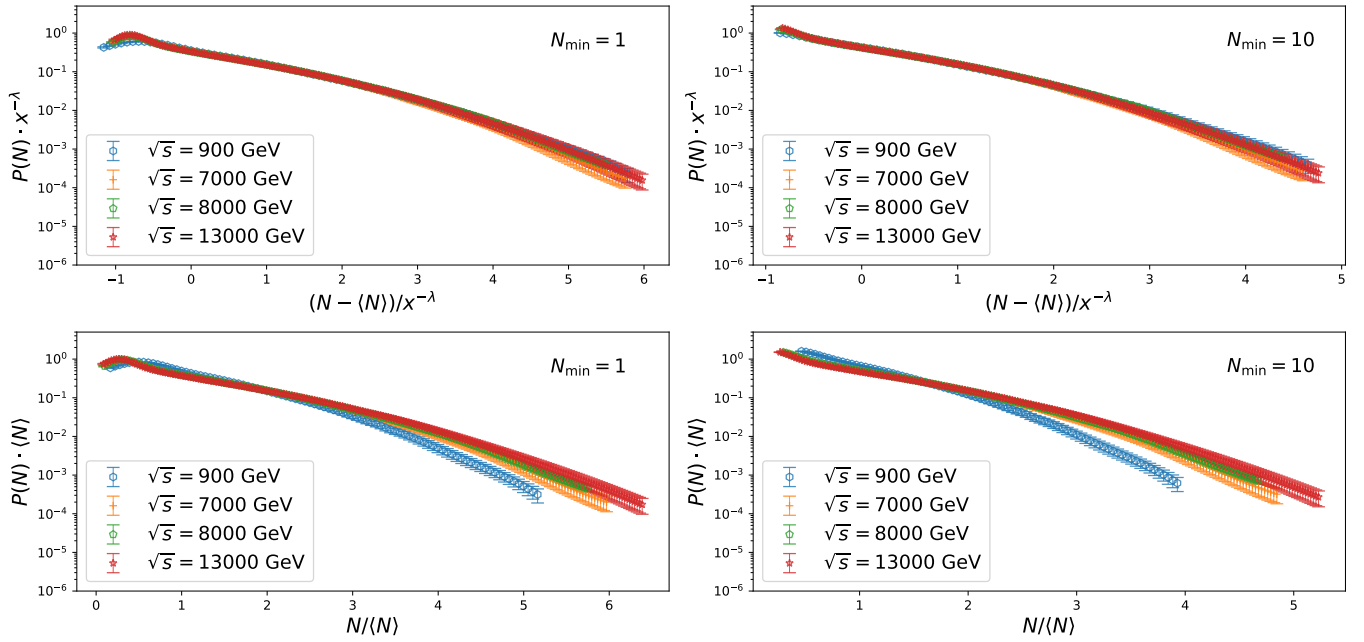


FIG. 6: Comparison between diffusion scaling (top) and KNO scaling (bottom) for two different values of  $N_{\min}$ . Data from ATLAS Collaboration [9, 23, 24], with  $|\eta| < 2.5$ .

ing form [36]:

$$\frac{\sigma_n}{\sigma_{\text{in}}} = \frac{\bar{N}}{\bar{N} + 1} P^{\text{NBD}}(1, \bar{N}, n), \quad (15)$$

where quantities  $N$  (with  $\bar{N} = N - 1$ ),  $\sigma_n$  and  $\sigma_{\text{in}}$  are the average multiplicity, the cross section for producing  $n$  hadrons, and the inelastic cross section, respectively.

The distribution of Eq. (15) is able to correctly describe the data at multiplicities  $n/\langle n \rangle \lesssim 4$  [35]. On the other hand, it overestimates the data for large multiplicities. In order to mitigate this shortcoming, an approach that sums all Pomeron diagrams (based on  $s$ -channel unitarity of the QCD Reggeon Field Theory) was considered [37]. The new multiplicity distribution now takes the form:

$$P_n = \frac{1}{N} \left[ 1 - \left( \frac{1}{N} \right)^{1-\gamma} \right]^{n-1}, \quad (16)$$

where  $\gamma$  is the dipole-dipole scattering amplitude in the Born approximation of pQCD.

After this correction, Eq. (16), the system of partons with large multiplicities is suppressed in relation to the distribution in Eq. (15) and LHC data are satisfactorily described [35]. The key point is that the distribution of Eq. (15) is obtained considering the creation of a dilute system of partons at central rapidities, whereas the distribution in Eq. (16) is related to a dense system of partons.

The final part of our analysis focuses on assessing the suitability of applying a fixed multiplicity cut at  $N_{\min} =$

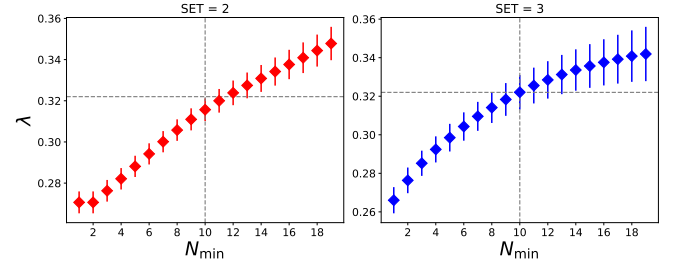


FIG. 7: The resulting  $\lambda$  from SET 2 and SET 3 considering different cuts in multiplicity  $N_{\min}$ .

10. To evaluate the impact of this choice on the extracted values of  $\lambda$ , we repeated the fit procedure across a range of  $N_{\min}$  values.

When low-multiplicity events are included (i.e., small  $N_{\min}$ ), the entropy growth rate is reduced, as expected from the dominance of soft processes and the slow increase of the total cross section in the absence of strong kinematic constraints. As we increase  $N_{\min}$ , the contribution of semi-hard and hard processes becomes more significant, leading to a faster entropy growth. This acceleration continues until a saturation point is reached around  $N_{\min} \sim 10$ , beyond which the growth rate stabilizes. This behavior is illustrated in Fig. 7, indicating that above this threshold, particle production exhibits a universal scaling with respect to the Bjorken- $x$  variable. This is also the point in which the values of  $\lambda$  extracted from LHC data are equal to the HERA given by (11).

## V. SUMMARY AND CONCLUSIONS

This work was driven by two central questions: whether a universal behavior governs charged hadron multiplicities across different high-energy collision systems—from HERA to the LHC—and whether the growth of the so-called scaling entropy exhibits universality rooted in initial-state QCD dynamics.

Our analysis demonstrates that, once low-multiplicity events are excluded, the entropy scaling observed in LHC data matches with remarkable precision the trends previously established in deep inelastic scattering at HERA. The extracted entropy growth rate, characterized by the parameter  $\lambda$ , is consistent across experiments and pseudorapidity windows, reinforcing the idea of a common underlying mechanism.

Moreover, we showed that at large multiplicities—where fluctuations are most significant—the multiplicity distributions obey a precise diffusion scaling. This behavior strongly suggests that the observed growth in entropy and variance with energy is not a consequence of final-state effects or hadronization, but rather reflects a universal scaling pattern associated with partonic dynamics in the initial state.

In conclusion, our findings support the existence of a universal entropy growth law and diffusion scaling behavior in high-energy hadronic collisions, bridging observations from  $ep$  scattering at HERA to  $pp$  collisions at the LHC. This provides further evidence that the most extreme multiplicity events encode fundamental information about the small- $x$  structure of hadrons and the dy-

namics of parton cascades.

Beyond its application to proton–proton collisions, the scaling entropy framework offers a valuable tool for disentangling initial- and final-state contributions in more complex systems, such as proton–nucleus and nucleus–nucleus collisions. Because entropy reflects early-stage partonic dynamics, it provides a clean observable largely insensitive to hadronization effects when analyzed above the soft-multiplicity threshold. This makes it a promising diagnostic for isolating initial-state physics in environments where final-state interactions, such as collective flow or quark-gluon plasma formation, are dominant.

Looking ahead, the scaling entropy method may also play an important role in future measurements at the upcoming Electron–Ion Collider (EIC), where precise control over the Bjorken- $x$  and  $Q^2$  kinematics will allow for stringent tests of universality and gluon saturation effects. Similarly, applying this framework to high-multiplicity events in heavy-ion collisions could help clarify which observables are rooted in initial-state structure versus those emerging from final-state dynamics.

## ACKNOWLEDGMENTS

MVTM acknowledges funding from the Brazilian agency Conselho Nacional de Desenvolvimento Científico e Tecnológico (CNPq) with the grant CNPq/303075/2022-8. F.S.N. gratefully acknowledges the support from the Fundação de Amparo à Pesquisa do Estado de São Paulo (FAPESP).

- 
- [1] ALICE, S. Acharya *et al.*, *Eur. Phys. J. C* **79**, 857 (2019), 1905.07208.
  - [2] ALICE, S. Acharya *et al.*, (2025), 2502.18081.
  - [3] B. Schenke, P. Tribedy, and R. Venugopalan, *Phys. Rev. C* **89**, 024901 (2014), 1311.3636.
  - [4] Z. Koba, H. B. Nielsen, and P. Olesen, *Nucl. Phys. B* **40**, 317 (1972).
  - [5] ALICE, J. Adam *et al.*, *Eur. Phys. J. C* **77**, 33 (2017), 1509.07541.
  - [6] A. Giovannini and R. Ugoccioni, *Phys. Rev. D* **59**, 094020 (1999), hep-ph/9810446, [Erratum: *Phys. Rev. D* **69**, 059903 (2004)].
  - [7] I. Zborovský, *Eur. Phys. J. C* **78**, 816 (2018), 1811.11230.
  - [8] CMS, V. Khachatryan *et al.*, *JHEP* **01**, 079 (2011), 1011.5531.
  - [9] ATLAS, G. Aad *et al.*, *New J. Phys.* **13**, 053033 (2011), 1012.5104.
  - [10] K. J. Golec-Biernat and M. Wusthoff, *Phys. Rev. D* **59**, 014017 (1998), hep-ph/9807513.
  - [11] A. M. Stasto, K. J. Golec-Biernat, and J. Kwiecinski, *Phys. Rev. Lett.* **86**, 596 (2001), hep-ph/0007192.
  - [12] M. Praszalowicz and T. Stebel, *JHEP* **03**, 090 (2013), 1211.5305.
  - [13] F. Gelis, R. B. Peschanski, G. Soyez, and L. Schoeffel, *Phys. Lett. B* **647**, 376 (2007), hep-ph/0610435.
  - [14] L. S. Moriggi, G. M. Peccini, and M. V. T. Machado, *Phys. Rev. D* **102**, 034016 (2020), 2005.07760.
  - [15] L. S. Moriggi, G. S. Ramos, and M. V. T. Machado, *Phys. Rev. D* **110**, 034005 (2024), 2405.01712.
  - [16] L. McLerran and M. Praszalowicz, *Phys. Lett. B* **741**, 246 (2015), 1407.6687.
  - [17] T. Osada and T. Kumaoka, *Phys. Rev. C* **100**, 034906 (2019), 1904.10823.
  - [18] T. Osada, *Phys. Rev. C* **103**, 024911 (2021), 2011.00456.
  - [19] M. Praszalowicz, *Phys. Lett. B* **727**, 461 (2013), 1308.5911.
  - [20] L. S. Moriggi and M. V. T. Machado, *Phys. Rev. D* **111**, 014017 (2025), 2412.16348.
  - [21] N. N. Nikolaev and B. Zakharov, *Z. Phys. C* **49**, 607 (1991).
  - [22] Y. L. Dokshitzer, V. A. Khoze, S. I. Troian, and A. H. Mueller, *Rev. Mod. Phys.* **60**, 373 (1988).
  - [23] ATLAS, G. Aad *et al.*, *Eur. Phys. J. C* **76**, 403 (2016), 1603.02439.
  - [24] ATLAS, M. Aaboud *et al.*, *Eur. Phys. J. C* **76**, 502 (2016), 1606.01133.



- [25] ALICE, S. Acharya *et al.*, Phys. Lett. B **845**, 138110 (2023), 2211.15326.
- [26] A. Dumitru and E. Petreska, (2012), 1209.4105.
- [27] F. Gelis, T. Lappi, and L. McLerran, Nucl. Phys. A **828**, 149 (2009), 0905.3234.
- [28] G. R. Germano, F. S. Navarra, G. Wilk, and Z. Wlodarczyk, Phys. Rev. D **110**, 034026 (2024), 2406.04856.
- [29] Y. Liu, M. A. Nowak, and I. Zahed, (2023), 2302.01380.
- [30] X.-P. Duan, L. Chen, G.-L. Ma, C. A. Salgado, and B. Wu, (2025), 2503.24200.
- [31] Y. L. Dokshitzer and B. R. Webber, (2025), 2505.00652.
- [32] E. Levin, Phys. Rev. D **111**, 016019 (2025), 2412.02504.
- [33] E. Levin, Eur. Phys. J. C **84**, 662 (2024), 2306.12055.
- [34] E. Gotsman and E. Levin, Eur. Phys. J. C **81**, 99 (2021), 2008.10911.
- [35] E. Gotsman and E. Levin, Phys. Rev. D **102**, 074008 (2020), 2006.11793.
- [36] D. E. Kharzeev and E. M. Levin, Phys. Rev. D **95**, 114008 (2017), 1702.03489.
- [37] A. Kovner, E. Levin, and M. Lublinsky, JHEP **08**, 031 (2016), 1605.03251.